Mater Renew Sustain Energy (2013) 2:7
DOI 10.1007/s40243-013-0007-0

REVIEW PAPER

Thermochemical hydrogen production from water using reducible oxide materials: a critical review

Lawrence D'Souza

Received: 17 September 2012 / Accepted: 3 January 2013 / Published online: 1 February 2013

Abstract This review mainly focuses on summarizing the different metal oxide systems utilized for water-splitting reaction using concentrated solar energy. Only two or three cyclic redox processes are considered. Particle size effect on redox reactions and economic aspect of hydrogen production via concentrated solar energy are also briefly discussed. Among various metal oxides system CeO_2 system is emerging as a promising candidate and researchers have demonstrated workability of this system in the solar cavity-receiver reactor for over 500 cycles. The highest solar thermal process efficiency obtained so far is about 0.4 %, which needs to be increased for real commercial applications. Among traditionally studied oxides, thin-film ferrites looks more promising and could meet US Department of energy target of \$2.42/kg H_2 by 2025. The cost is mainly driven by high heliostat cost which needs to reduced significantly for economic feasibility. Overall, more work needs to be done in terms of redox material engineering, reactor technology, heliostat cost reduction and gas separation technologies before commercialization of this technology.

Keywords Hydrogen · Water splitting · Solar thermal

Introduction

Hydrogen is considered as next generation fuel to propel airplanes, automotive vehicles and virtually any stationary power system using fuel cells. The non-polluting by-product 'water' upon hydrogen combustion has attracted world attention to save ever polluting earth environment for sustainable future. Currently, the hydrogen is derived from fossil fuels. The smallest molecule of universe sees highest demand due to its non-polluting end product as well as its remarkable chemical and physical properties. There are number of chemical transformation in which hydrogen is used as hydrogenating or reducing agent. Moreover, present trend to harvest CO_2 into useful chemicals demands hydrogen. Many scientists around the world are pessimistic about CO_2 hydrogenation since they see raising demand for hydrogen and currently there are no real alternatives to fulfill other than fossil fuels. Researchers have been looking at different possibilities to generate hydrogen by biological and chemical means. Electrolysis of water is one of the easy and greener route to generate hydrogen only if electricity comes from wind, tidal, photovoltaics, geothermal or hydropower. The other greener routes are photoelectrochemical water splitting [1], by direct splitting of water [2, 3] and solar thermochemical cycles. It is hoped that combination of several technologies can fulfill future hydrogen demand.

Water splitting by low valent metal oxides at high temperature is one of the clean way of hydrogen production since the temperature needed to perform chemical reaction comes from concentrated solar thermal heat. Though the technology is known since more than three decades commercial realization is yet to happen due to numerous challenges in this technology. The off-sun hours, cloudy and rainy seasons are main drawbacks for commercial realization. Moreover, technology cannot be implemented in geographically poor sun receiving regions.

This review summarizes the work done in high-temperature hydrogen production via two-step redox processes

L. D'Souza (✉)
SABIC Corporate Research and Innovation Center (CRI) at KAUST, Saudi Basic Industries Corporation, P.O. Box 4545-4700, Thuwal 23955-6900, Saudi Arabia
e-mail: dsouzal@sabic.com

using various metal oxides (Table 1). Only the high-temperature experiments demonstrated either in solar furnace or in laboratory fixed-bed reactor have been considered. This review does not cover the hybrid technologies or other forms of hydrogen production technologies.

Bilgen et al. [4] have demonstrated the possibility of splitting water directly at high temperature. The theoretical calculation for the said reaction is depicted in Fig. 1. It was found that the amount of hydrogen produced decreases with increase in H_2O partial pressure. Figure 1 gives the compounded results for partial pressure of water equal to 0.1 bar between 1,500 and 5,000 K. Bilgen [4] experimentally demonstrated that between 2,273 and 2,773 K formation of about 2–3 % H_2 when mixture of steam and argon was passed in the crucible at the focus of the solar furnace.

The dissociation of metal oxide to their respective metal is written as follows [14]:

$$M_xO_y = xM + \frac{y}{2}O_2. \quad (1)$$

The temperature required for few metal oxides conversion to their metallic form is given in Table 2. Except for ZnO, achieving temperature needed to reduce metal oxide to their metallic form is practically impossible due to the high temperature required. Concentration ratios of up to 10,000 suns have been achieved by researchers which translate to 3,800 K. But high-temperature operation, reactor material thermal stability and radiation heat losses makes the process almost impossible. The temperature required to attain ΔG° of the reaction (1) equals zero can be substantially brought down by the use of hydrocarbon as reducing agents, for example graphite or methane, which can be written as follows:

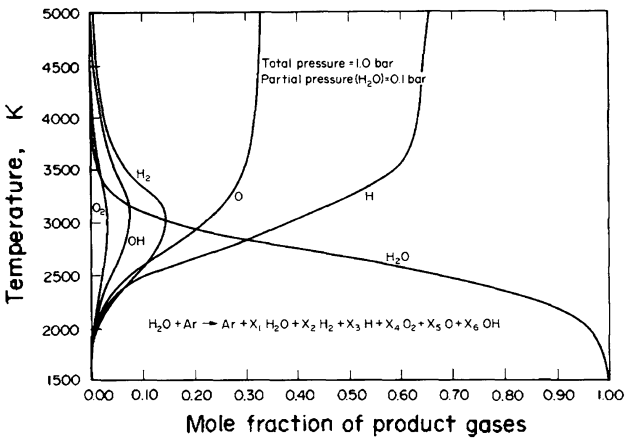

Fig. 1 Theoretical composition of the different products in the dissociation of water at high temperature; total pressure is 1 bar and partial pressure of H_2O is 0.1 bar

$$M_xO_y + yC(gr) = xM + yCO \quad (2)$$

$$M_xO_y + yCH_4 = xM + y(2H_2 + CO). \quad (3)$$

Two-step cyclic redox processes are simplest way of producing hydrogen by utilizing metal oxide. The solar reduction step is endothermic and can be written as shown in (4),

$$\frac{1}{\Delta\delta}M_xO_{y-\delta_{ox}} \rightarrow \frac{1}{\Delta\delta}M_xO_{y-\delta_{red}} + 0.5O_2 \quad (4)$$

$$\frac{1}{\Delta\delta}M_xO_{y-\delta_{red}} + H_2O \rightarrow \frac{1}{\Delta\delta}M_xO_{y-\delta_{ox}} + H_2 \quad (5)$$

$$\frac{1}{\Delta\delta}M_xO_{y-\delta_{red}} + CO_2 \rightarrow \frac{1}{\Delta\delta}M_xO_{y-\delta_{ox}} + CO \quad (6)$$

(where δ is non-stoichiometric coefficient and $\Delta\delta$ is change in non-stoichiometric coefficient).

The reaction (4) takes place at temperature above 1,000 K and many metal oxide systems have been studied over the past four decades. Several two- and three-step H_2O-splitting thermochemical cycles based on metal oxides redox reactions have been reported in the literature. Nakamura [5] first proposed the two-step redox cycle in 1977 for Fe_3O_4/FeO redox cycle; interest then diminished for the next two decades and thereafter a spurt of interest resulted in investigation of several other oxide systems for thermochemical redox cycle for hydrogen generation. The high temperature required for reduction reaction can be supplied by either concentrated solar energy or fossil fuels. The solar reduction is usually carried out in the presence of an inert gas, if a reducing gas is used the reduction temperature can be brought down substantially. The reduced metal oxide can be oxidized back to the original state by oxidants like H_2O or CO_2. If H_2O is used H_2 can be produced and if CO_2 is used CO can be produced as shown in Eqs. (5) and (6), respectively. If H_2O and CO_2 are used to oxidize the redox material alternatively or together one can produce the synthesis gas ($CO + H_2$) from totally renewable sources (CO_2 and H_2O) [30].

Sibieude et al. [10] demonstrated reduction of Fe_3O_4 to FeO in a solar furnace by heating the material 300 °C above its melting point. They could obtain up to 40 % conversion in air and 100 % conversion in argon atmosphere. Figure 2 gives the conversion rate of Fe_3O_4 to FeO as a function of temperature under argon flow (20 l/h).

As observed by many researchers, they also experienced that quenching the reduced oxides is very important. Table 3 summarized the FeO yield with various quenching rates. It can be seen that in presence of air up to 40 % conversion can be obtained with 373 K/s cooling rate.

As per literature the reduction of Mn_3O_4 to MnO occurs above 1,773 K [31]. Sibieude et al. [10] have studied reduction of Mn_3O_4 to MnO in a solar furnace. They could

Table 1 Summary of potential two-step water-splitting reaction systems reported in the literature

Main theme	T (K) for $\Delta G^0 = 0$	T (K) for reduction	H_2 yield (%)	T (K) for oxidation	References
$Fe_3O_4 = 3FeO + 1/2\ O_2$		2,500		<1,000	[5]
$2Mn_3O_4 = 6MnO + O_2$	2,000	1,810	0.002	900	[6]
$2\ Co_3O_4 = 6CoO + O_2$	1,000	1,175	4×10^{-7}	900	[6]
$2\ Nb_2O_5 = 4NbO_2 + O_2$	4,000	3,600	99.7	900	[6]
$ZnO = Zn + 1/2\ O_2$	2,350	2,300	Na	Na	[7–9]
Mn_3O_4 to MnO	Na	1,773	Na	Na	[10]
$(Fe_{1-x}M_x)_3O_4 = (Fe_{1-x}Mn_x)O$	Na		Very low	773–1,173	[11, 12]
$(Fe_{1-x}M_x)_3O_4 = (FeM)O$, M = Ni, Mn, Zn	Na	>1,073	Na	<1,073	[13]
$(Fe_{1-x}Mx)_3O_4 = (FeM)O$, M = Mn, Co, Mg	Na		Na	Na	[14]
$2CdO = 2Cd + O_2$	Na	>1,473	Na	Na	[10]
$SnO_2 = Sn + O_2$	Na	>1,873	90 %	773–873	[4, 15]
$ZnFe_2O_4 = Zn_xFe_{3-x}O_4$, Zn(g), O_2	Na	1,173			[16]
$x/3Fe_3O_4 + Y_yZr_{1-y}O_{2-y/2} = Fe_xY_yZr_{1-y}O_{2-y/2+x} + x/6\ O_2$	Na	1,673	Na	<1,273	[17, 18]
$Fe_xY_yZr_{1-y}O_{2-y/2+x} + x/3H_2O = x/3Fe_3O_4 + Y_yZr_{1-y}O_{2-y/2} + x/3H_2$					
$2CeO_2(s) = Ce_2O_3(s) + 1/2O_2(g)$; $Ce_2O_3(s) + H_2O(g) = 2CeO_2(s) + H_2(g)$	Na	2,273	Na	673–873	[19–21]
$Ce_{1-x}Zr_xO_2$ $(0 \le x \le 0.3)$	Na	1,773	Na	Na	[22–24]
$TiO_2 = TiO_x$, $x = 1.83$–1.96	Na	2,573–3,073	Na	Na	[25]
$2\ SiO_2 = 2\ SiO + O_2$	Na	3,250[a]	Na	2,729	[4, 26]
$SiO\ (g) + H_2O + SiO_2 + H_2$					
$WO_3\ (s) = W + 3/2\ O_2$	Na	4,183[a]	Na	1,157	[4, 26]
$W + 3H_2O = WO_3\ (s) + 3H_2$					
$MoO_2 = Mo + O_2$	Na	3,986[a]	Na	1,816	[4, 26]
$Mo + 2H_2O = MoO_2\ (s) + 2H_2$					
$3\ In_2O_3 = In_2O_3 + 4\ In$	Na	>2,780[a]	Na	1,000	[4]
Solid acids viz. SiO_2, Al_2O_3, TiO_2, ZnO, $CaCO_3$	Na	Na	Na	Na	[27]
$In_2O_3 = In_2O + O_2$ $In_2O + 2H_2O = In_2O_3 + H_2$	Na	2,473	Na	1,073	[28]
$MnFe_2O_4 + 3CaO + (1 - y)H_2O = Ca_3(Fe,Mn)_3O_{8-y} + (1 - y)H_2$ $Ca_3(Fe,Mn)_3O_{8-y} = MnFe_2O_4 + 3CaO + (1 - y)/2\ O_2$	Na	1,273	Na	873	[29]

Na data not available

[a] Process is practically not feasible

Table 2 Approximate temperature required for which $\Delta G°$ of the reaction (1) equals zero

Metal oxide	T (K) for $\Delta G^0 = 0$
Fe_2O_3[a]	3,700
Al_2O_3	>4,000
MgO	3,700
ZnO	2,335
TiO_2[a]	>4,000
SiO_2[a]	4,500
CaO	4,400

[a] Fe_2O_3, TiO_2 and SiO_2 decompose to lower valence oxides before complete dissociation to the final

obtain about 80 % conversion at 2,173 K under atmospheric pressure of air with a cooling rate of 373 K/s. The quenching of the MnO is very important to stop backward reaction, i.e., formation of Mn_3O_4 again. They have not performed more extensive work on this system.

Ehrensberger et al. [11] have studied non-stoichiometric FeMn oxides for two-step water-splitting reaction. They calculated ΔG_R values for two-step Nakamura cycles FeO–Fe_3O_4 and MnO–Mn_3O_4 and the plotted results are shown in the Figs. 3, 4. Figure 3 indicates that ΔG^0 equals to zero for the reduction of Mn_3O_4 to MnO is at least 500 K less than that of Fe_3O_4 to FeO system. However, Fig. 4 indicates that FeO can produce hydrogen between 873 and 1,073 K but MnO system is unable to produce hydrogen in significant levels. This led the authors to think of the possibility of combining Fe and Mn oxides to reduce spinel at lower temperature as well as produce hydrogen in significant amount in oxidation step. Authors demonstrated the oxidation of $Fe_{1-y}O$ and $(Fe_{1-x}Mn_x)_{1-y}O$ $(x \le 0.3)$ in a laboratory tubular furnace and monitored gaseous

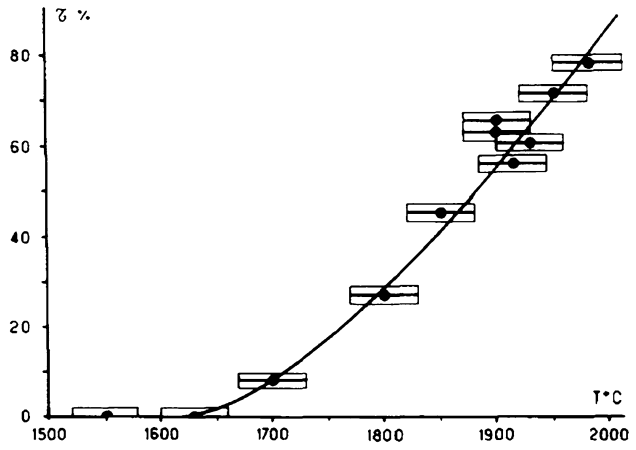

Fig. 2 Conversion rate of magnetite versus temperature

Table 3 Influence of cooling rate on FeO yield in air and argon atmosphere

Atmosphere	Quenching speed (K s^{-1})	%mol FeO
Air[a]	278	0
	293	25
	373	40
	1,273	50
Argon[a]	278	40
	293	45
	373	55
	1,273	60

[a] Residence time = 1 min, temperature = 2,173 K, flow rate = 20 l/h

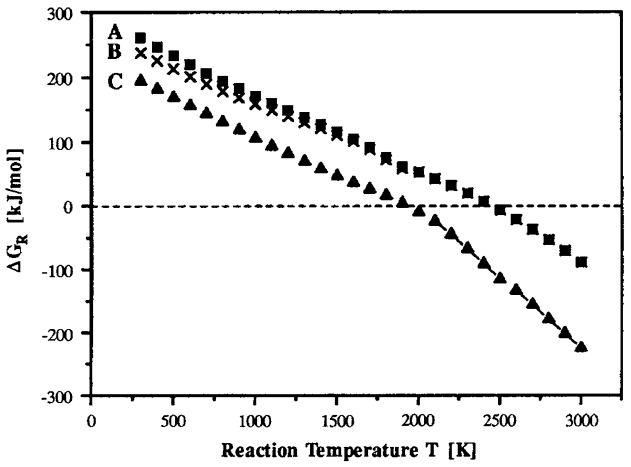

Fig. 3 Gibbs free enthalpy ΔG_R for the decomposition of Fe_3O_4 (*A*, *B*) and Mn_3O_4 (*C*) to FeO (*A*), $Fe_{0.947}O$ (*B*) and MnO (*C*) as a function of temperature

products using mass spectrometer. At atmospheric pressure, water with a partial pressure of about 4,200 Pa in nitrogen was able to oxidize $(Fe_{1-x}Mn_x)_{1-y}O$ ($x = 0.0$, 0.1, 0.3) to $(Fe_{1-x'}Mn_{x'})_3O_4$ with $x' < x$ forming molecular hydrogen. The substitution of iron with 10–30 % Mn in the wuestite phase did not lower the total amount of hydrogen formed, but it changed the kinetics of the process significantly. It was also found that the process is thermodynamically controlled at high temperature. The rate of water splitting decreased with increase in manganese concentration.

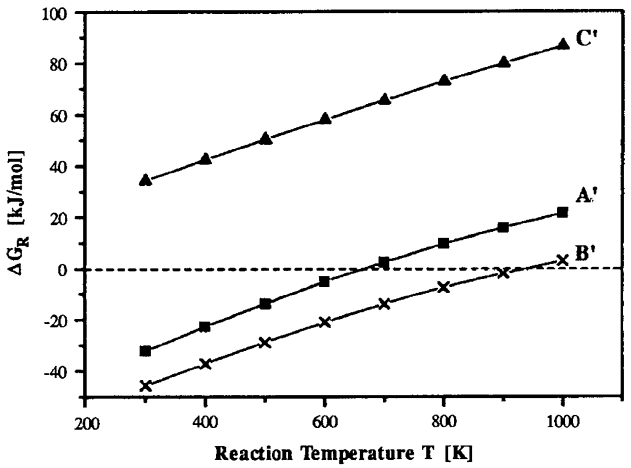

Fig. 4 Gibbs free enthalpy ΔG_R for the water splitting reaction of FeO (*A'*), $Fe_{0.947}O$ (*B'*) and MnO (*C'*) as a function of temperature

They also found that during water-splitting reaction $(Fe_{1-x}Mn_x)_{1-y}O$ forms manganese-rich rock salt phase and an iron-rich spine phase due to phase segregation processes [12].

Tamura et al. [13] extended the work to 'NiMnFe' system, as shown in the reaction schemes 7 and 8.

$$Ni_{0.5}Mn_{0.5}Fe_2O_4 \xrightarrow[\text{at} > 1{,}073\ \text{K}]{\text{activation}} Ni_{0.5}Mn_{0.5}Fe_2O_{4-\delta} + \frac{\delta}{2}O_2 \quad (7)$$

$$Ni_{0.5}Mn_{0.5}Fe_2O_{4-\delta} + \delta H_2O \xrightarrow[\text{at} < 1{,}073\ \text{K}]{\text{water-splitting}} Ni_{0.5}Mn_{0.5}Fe_2O_4 + \delta H_2 \quad (8)$$

They performed the above two-step reaction in a solar reactor at 1,073 K. In the first endothermic step, $Ni_{0.5}Mn_{0.5}Fe_2O_4$ was thermally activated to get oxygen-deficient compound, in the second step the oxygen-deficient compound was oxidized using H_2O to produce H_2. Since, O_2 and H_2 were produced in two different steps, high-temperature separation of those gases can be eliminated in the proposed method. They have demonstrated the workability of two-step water-splitting reaction with $NiFe_2O_4$, $Ni_{0.5}Mn_{0.5}Fe_2O_4$ and $Ni_{0.5}Zn_{0.5}Zn_2O_4$ systems using thermogravimetric experiments. They found that $NiFe_2O_4$ system needs lower reactivation rate (conducted after the water-splitting reaction) compared to

$Ni_{0.5}Mn_{0.5}Fe_2O_4$ system. The oxygen released during reduction step in $NiFe_2O_4$, $Ni_{0.5}Mn_{0.5}Fe_2O_4$ and $Ni_{0.5}Zn_{0.5}Zn_2O_4$ systems were 0.2, 0.3 and 0.4 %, respectively. They also demonstrated the workability of the two-step hydrogen production in solar reactors. They performed two redox cycles to prove the oxygen and hydrogen evolution in activation (reduction) and reactivation (oxidation) processes. The activation was conducted at 1,373 K in presence of Ar and reactivation was conducted in presence of (steam + Ar) flow at 573 K. In the case of $ZnFe_2O_4$, reduction follows two pathways [16] as shown in Eqs. 9 and 10.

$$3ZnFe_2O_4 = 3Zn + 2Fe_3O_4 + 2O_2 \quad (9)$$

$$6ZnFe_2O_4 = 6ZnO + 4Fe_3O_4 + O_2 \quad (10)$$

The reduction and oxidation steps have been demonstrated using Xe beam experiment and solar furnace experiments. It took less than 60 s for the Zn-ferrite to release the expected amount of O_2 from the lattice at 1,750 K. Authors have seen deposition of Zn on the reactor walls during reduction step and have measured O_2 released using mass spectrometer.

Abanades et al. [19] examined CeO_2/Ce_2O_3 redox pairs and demonstrated the feasibility in a solar reactor featuring an inert gas atmosphere at $T = 2{,}273$ K, $P = 100$–200 mbar. It consists of two chemical steps: (1) reduction, $2CeO_2 \rightarrow Ce_2O_3 + 0.5O_2$; (2) hydrolysis, $Ce_2O_3 + H_2O \rightarrow 2CeO_2 + H_2$. The reduction step is endothermic and takes place at $T = 2{,}273$ K, $P = 100$–200 mbar; however, oxidation step takes place at 673–873 K resulting in pure hydrogen which can be directly used in fuel cells application. The main advantages of the process are low cost material which is abundantly available in nature and the process uses non-corrosive chemicals. The reduced phase is very stable at ambient temperature and nonreactive to moisture and oxygen which makes this material ideal for on-site hydrogen generation which in turn overcomes problem associated with transportation. However, this technology has few drawbacks, a maximum heat input temperature slightly higher than 2,273 K, the cycle working temperature of the endothermic step must be optimized to be compatible with dish or tower technologies, and to reduce sample vaporization. High molecular weight of cerium oxides poses problem in the flow of solids in the process.

Chueh et al. [20] have extended the work on CeO_2 system. They demonstrated the O_2 evolution during reduction step, CO and H_2 generation during oxidation step using the solar cavity-receiver reactor over 500 cycles. They could achieve solar-to-fuel efficiencies of 0.7–0.8 % and concluded that efficiency is limited by the system scale and design rather than by chemistry. However, Rager [32] pointed out that the efficiency 0.7–0.8 % efficiency refers to 'peak instantaneous efficiency' but after averaging the efficiency over 80 % of the fuel production, the actual efficiency is just 0.4 %. He recalculated the solar thermal process efficiency and found that the value is still lower than that of reported by Chueh et al. [20], mainly because the later authors did not consider the energy need for large amount of purge gas used in redox processes. Purge gas takes up lot of solar heat and hence results in lower solar thermal efficiency.

Kang et al. [23] have extended the work on CeO_2 system. They synthesized $Ce_xZr_{1-x}O_2$ ($x = 0.6, 0.7, 0.8, 1.0$) solid solutions and tested for redox reactions. They found that the reduced $Ce_xZr_{1-x}O_{2-\delta}$ ($x = 0.5, 0.6, 0.7, 0.8, 1.0$) samples exhibited higher hydrogen production ability for water splitting due to improved oxygen diffusion through the bulk. Kaneko et al. [22] have extended the work on $Ce_xZr_{1-x}O_{2-\delta}$ solid solution system. They introduced Zr^{4+} on various ratios in CeO_2 lattices and found that the oxygen releasing capacity or extent of CeO_2 reduction increases with the increase of Zr^{4+} ions similar to Kang et al.'s [23] observations. The highest oxygen release was found at $x = 2$ ($Ce_{0.8}Zr_{0.2}O_2$) at 1,773 K in air and the amount of reduced cerium was found to be about 11 % which is seven times higher than just with bare CeO_2. The enhancement of the O_2-releasing reaction with CeO_2–ZrO_2 oxide is found to be caused by an introduction of Zr^{4+}, which has smaller ionic radius than Ce^{3+} or Ce^{4+} in the fluorite structure.

Le Gal and Abanades [24] doped trivalent lanthanides, viz. La, Sm and Gd in CeO_2 to form binary oxides and used in hydrogen production by solar thermal redox cycles. They found that trivalent lanthanide-doped material improves the thermal stability of the material during consecutive redox cycles, but hydrogen production remains the same as ceria. They also doped trivalent lanthanides in CeO_2–ZrO_2 to form ternary oxides. They found that with 1 % gadolinium to ceria–zirconia solid solutions nearly 338.2 μmol of hydrogen per gram during one cycle with the O_2-releasing step at 1,400 °C and the H_2-generation step at 1,050 °C. This quantity of hydrogen is more than with CeO_2–ZrO_2 system. They also found that the addition of lanthanum enhances the thermal stability of ceria–zirconia solid solution similar to as observed in cases of lanthanum-doped CeO_2 binary oxides.

Lipinski et al. [21] applied first and second laws of thermodynamics to analyze the potential of applying heat recovery for realizing high efficiency in solar-driven CeO_2-based non-stoichiometric redox cycles to split H_2O or CO_2. They found that at 2,000 K, with 80 % solid phase heat recovery, advanced materials can only increase efficiency from 16 to 20 %, while, at 1,850 K, advanced materials can improve efficiency from 14 to 23 %, a higher maximum value because of decreased re-radiation and gas heating at the lower value of T_{red}.

Inoue et al. [33] demonstrated effectiveness of a ZnO/$MnFe_2O_4$ system in a lab furnace at 1,273 K. When H_2O was contacted with ZnO/$MnFe_2O_4$ at 1,273 K H_2 formation happens with the expense of oxidation of ZnO/$MnFe_2O_4$. The later forms spinel kind of material containing Zn^{II}, Mn^{II}, Mn^{III} and Fe^{III} ions. The reaction happens by incorporation of Zn^{II} ions into $MnFe_2O_4$ crystal structure, accompanied by the partial oxidation of Mn^{II} in $MnFe_2O_4$ to Mn^{III}. The second step, oxygen releasing can be carried out using solar thermal route but this is not demonstrated experimentally by authors. Similarly, they have also demonstrated H_2 production using CaO (or Na_2CO_3) and $MnFe_2O_4$ by passing steam at 1,273 K [29]. The mechanism of H_2 formation is similar to that explained earlier, i.e., oxidation of Mn^{II} to Mn^{III} to form spinel kind of material ($Ca_3{}^{2+}Fe^{3+}_{2.02}Mn^{2+}_{0.96}Mn^{3+}_{0.02}O_{7.02}$).

Roeb et al. [34] used monolith coatings for redox system. They noticed that the potential of the monolith coatings to absorb oxygen from steam and to release hydrogen decreased with the number of completed cycles which is due to sintering of the material which increases with the redox cycles.

Lundberg [6] performed computer model calculation for various systems for two-step solar hydrogen productions, the systems considered were CoO/Co_3O_4, MnO/Mn_3O_4, FeO/Fe_3O_4, NbO_3/Nb_2O_5 and the halide systems FeX_2/Fe_3O_4 where $X = F, Cl, Br$ and I. In his calculation he found that the ratio of H_2/H_2O is controlled by the temperature and oxygen partial pressure generated by the redox system. The yield of the hydrogen is defined as follows:

$$Y\ (\%) = \frac{H_2(\text{formed})}{H_2(\text{max})} \times 100 \tag{11}$$

where H_2max is the maximum amount of hydrogen that can be formed as per the formula:

$$MO(\text{red}) + H_2O(g) = MO(\text{ox}) + H_2(g). \tag{12}$$

Calculations showed that FeO–Fe_3O_4 and NbO_2–Nb_2O_5 systems give more H_2 yield at lower temperature and that of MnO–Mn_3O_4 and CoO–Co_3O_4 systems give >1 % H_2 yield at any temperature. In reduction step, in order to reduce thermally oxidized metal oxide needs to be heated up to a temperature where its oxygen partial pressure is higher than in atmosphere (0.21 atm). It was found that though FeO–Fe_3O_4 and NbO_2–Nb_2O_5 give higher yield they need to be heated above their melting point to reduce them. On the other hand, MnO–Mn_3O_4 and CoO–Co_3O_4 systems can be reduced below their melting point but hydrogen yield in these systems are very low (Table 4). Therefore, none of the systems studied are suitable to fulfill both desired conditions for the redox reactions.

It was also tried to combine metal oxide which yields higher H_2 with metal oxide which can be reduced below its melting point to find out whether this fulfills the need of redox cycle. Considering the spinel phase composition of $(Fe_{0.85}Co_{0.15})_3O_4$ the H_2 yield obtained was 45 %, but during the oxidation of the $(Fe_{0.85}Co_{0.15})O$ system the equilibrium oxygen pressure of the redox system will successfully increases and the yield of the H_2 will gradually decreases down to about 3 %. The opposite effect was found during the reduction step, the spinel phase with composition $(Fe_{0.85}Co_{0.15})_3O_4$ will start to be reduced at 2,020 K, but while reduction of the spinel the wuestite phase will become rich with iron and the oxygen partial pressure will decrease leading to gradual increase in the reduction temperature of 2,135 K by the time the initial composition is reached.

An yttrium-stabilized cubic zirconia material coated with iron oxide was proposed to split water in the temperature range 1,273–1,673 K [35, 36]. Kodam et al. [17] studied supported Fe_3O_4–FeO system. Various amount of iron oxide was supported on yttrium-supported ZrO_2 for cyclic redox study. It was found that the Fe_3O_4 reacts with YSZ to produce Fe^{2+}-containing ZrO_2 phase by releasing oxygen molecules in the first step. It was also found that the Fe^{2+} ions enters into the cubic YSZ lattice. In the second step, the Fe^{2+}-containing YSZ generated hydrogen via steam splitting to reproduce Fe_3O_4 on the cubic YSZ support. The system showed good reproducibility. It was found that when the Fe_3O_4 content was increased up to 30 wt% on the Fe_3O_4/YSZ sample [17], the sample became denser and harder mass after the thermal reduction step, similar to the unsupported Fe_3O_4. This is due to the fact that the limitation of Fe^{2+} solubility in the YSZ exists close

Table 4 The yield of H_2 at 900 K for the different metal oxide systems together with the enthalpy of the reaction, the reduction temperature in air and the melting points of the system

System	Yield H_2 at 900 K (%)	$\Delta H_r/H_2$ at 900 K (kJ)	Reduction temperature in air	Melting point (K)	
				Reduced phase	Oxidized phase
NbO_2/Nb_2O_5	99.7	−62.7	3,600	2,175	1,785
FeO/Fe_3O_4	63	−49.5	2,685	1,650	1,870
MnO/Mn_3O_4	0.002	17	1,810	2,115	1,835
CoO/Co_3O_4	4×10^{-7}	251.2	1,175	2,080	Decomposes at 1,175

to the 25 wt% Fe_3O_4 content in the Fe_3O_4/YSZ. When raising the Fe_3O_4 content above 25 wt%, excess Fe^{2+} ions would form FeO crystals on the ZrO_2 surface, which in turn melts at 1,713 K. Therefore, the Fe_3O_4 contents should be limited to <25 % to avoid sintering of redox material and its cyclic reproducibility.

The disadvantage of mixed iron oxide cycles where oxides are partially reduced and oxidized is their low molar ratio of released oxygen to the total oxygen present in the system. The major drawback of all systems using reactive coatings is their low ratio of hydrogen mass generated to support structure mass. Considering the properties of the above problems, the cycle based on the ZnO/Zn redox pair [7–9] is of special interest since no cyclic heating and cooling is required and a pure metal state is achieved. It consists of the solar endothermal dissociation of ZnO(s) into its elements; and the non-solar exothermal steam-hydrolysis of Zn into H_2 and ZnO(s), and represented by Eqs. 13 and 15.

$$\text{1st step (solar ZnO-decomposition)}: \mathrm{ZnO} \rightarrow \mathrm{Zn} + 0.5\mathrm{O_2} \tag{13}$$

$$\text{2nd step (non-solar Zn-hydrolysis)}: \mathrm{Zn} + \mathrm{H_2O} \rightarrow \mathrm{ZnO} + \mathrm{H_2} \tag{14}$$

H_2 and O_2 are derived in different steps, thereby eliminating the need for high-temperature gas separation. This cycle has been proposed to be a promising route for solar H_2 production from H_2O because of its potential of reaching high-energy conversion efficiencies and thereby its economic competitiveness [37, 38].

The first step of the two-step ZnO/Zn water-splitting cycle was first demonstrated in a solar furnace in 1977 by Bilgen et al. [4]. They have demonstrated the decomposition of ZnO in a solar furnace. They also found that Zn yield increases if ZnO is diluted with other refractory materials like ZrO_2 and Y_2O_3 and if the reaction is carried out in the presence of argon inert gas. Table 5 summarized the Zn yield found in the different experiments and different conditions.

Recently, the solar thermal ZnO dissociation was demonstrated by Lédé et al. [39] in a quartz vessel containing sintered ZnO, by Haueter et al. [40] in a rotating cavity reactor type, and by Perkins et al. [41] in an aerosol reactor type. Perkins et al. reported the O_2 measurement, which is the only clear indicator of the ongoing thermal ZnO dissociation. The maximum net Zn yield was 17 % [41]. However, to-date there is no report in the literature which claims continuous dissociation of ZnO monitored by product gas analysis for more than few minutes.

Palumbo et al. [25] have studied TiO_2 system for two-step solar production of Zn from ZnO, the primary reaction schemes can be written as shown in reactions (15) and (16).

$$\mathrm{TiO_2(l)} = \mathrm{TiO(l)} + (1 - x/2)\mathrm{O_2} \quad T \geq 2,300\ \mathrm{K} \tag{15}$$

$$\mathrm{TiO}_x\mathrm{(s,l)} + (2 - x)\mathrm{ZnO(s)} = (2 - x)\mathrm{Zn(g)} + \mathrm{TiO_2(s)} \quad T > 1,200\ \mathrm{K} \tag{16}$$

But the authors have not tried water splitting using partially reduced TiO_x. The minimum values of x that the authors obtained experimentally were 1.91, 1.86 and 1.83 for temperatures of 2,300, 2,500, and 2,700 K, respectively, in an Ar atmosphere at 1 bar. They used the latter material to reduce ZnO to produce Zn as indicated in reaction (16). It is to be noted that the higher the degree of decomposition, the greater the vaporization of TiO_2, this limits the efficiency of the water-splitting cycle using TiO_2 system.

Sibieude et al. [10] have used CdO for two-step water-splitting reaction. They demonstrated reduction of CdO to Cd in a solar furnace at high temperature. The reaction scheme is shown in Eqs. 17–19.

Table 5 Mol% zinc content of condensed vapors from ZnO and mixed oxides ZnO–Y_2O_3, ZnO–ZrO_2 samples heated at the focus of 2 kW solar concentrator

	Air p (bar)		Argon atmosphere p (bar)					
	<0.001	1	<0.001	0.034	0.092	0.263	0.789	
ZnO	Between 20 and 30 mol% of Zn	No Zn formation	Difficulties exist in obtaining due to strong volatilization of ZnO sample; the results are poorly reproducible					Static atmosphere
			68 mol% was obtained for $p < 0.001$ bar Ar					
			45 mol% was obtained for $p = 0.263$ bar Ar (in a flow of gas)					
10 mol% ZnO				70 %	62 %	60 %	25 %	Static atmosphere
90 mol% Y_2O_3			71 %	76 %	66 %	68 %	65 %	Gas circulation
10 mol% ZnO				67 %	60 %	60 %	30 %	Static atmosphere
90 mol% ZrO_2			75 %	74 %	65 %	70 %	67 %	Gas circulation

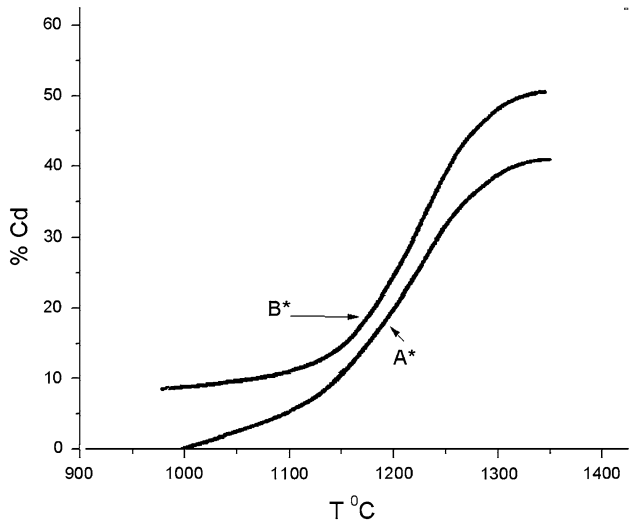

Fig. 5 Cd (metal) content of condensates versus temperature after thermal decomposition of CdO, flow rate of argon was A^* 3.4 cm^3/s and B^* 10 cm^3/s

$$CdO \rightarrow Cd + {}^1/_2O_2 \quad T > 1,200\ ^\circ C \tag{17}$$

$$Cd + H_2O \rightarrow Cd(OH)_2 + H_2 \tag{18}$$

$$Cd(OH)_2 \rightarrow CdO + H_2O \quad T > 375\ ^\circ C \tag{19}$$

They observed that subjecting CdO alone to solar radiation did not reduce the oxide, but when CdO was mixed with refractory material, in their case 20 %mol ZrO_2, resulted in the formation of Cd metal in the stream of Ar. The amount of Cd metal in the deposited condensate at different temperatures is shown in Fig. 5.

Quenching of evaporated metal was very important in this reaction. When CdO was dissociated into Cd(g) and O(g) the recombination will also takes place very fast.

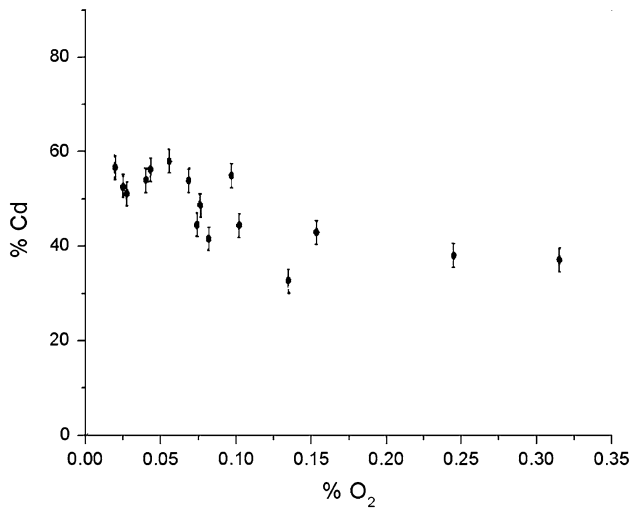

Fig. 6 Dependence of Cd (metal) content of condensates on the oxygen concentration of the argon flow

When CdO alone was heated strong vaporization produces large amount of dissociated vapors which is insufficiently quenched by the argon flow on a water cooled wall of the condenser. The problem was overcome by mixing the CdO with ZrO_2; in this case vaporization rate of Cd metal was lowered by its dispersion in the refractory metal oxide matrix which permits the effective quenching of vaporized metal. It is to be noted that partial pressure of oxygen plays a main role in the Cd yield. Figure 6 gives the %Cd metal recovered in various O_2 partial pressures.

Abanades et al. [15] have studied $SnO_2 = Sn + 1/2O_2$ cycle which consists of a solar endothermic reduction of SnO_2 into SnO(g) and O_2 followed by a non-solar exothermic hydrolysis of SnO(s) to form H_2 and SnO_2(s).The thermal reduction occurs under atmospheric pressure at about 1,873 K and over. The solar step encompasses the formation of SnO nanoparticles that can be hydrolyzed efficiently in the temperature range of 500–600 °C with a H_2 yield over 90 %. A preliminary process design is also proposed for cycle integration in solar chemical plants. They also compared their system with literature reported 'Sn-Souriau' [42] three-step cycles and inferred that the reaction (22) producing hydrogen from the Sn/SnO_2 mixture produced from reaction (21) is slow and partial at 600 °C which results in low H_2 yield of <45 %. The three-step cycling process proposed by them is as follows:

$$SnO_2 \rightarrow SnO + 1/2O_2 \tag{20}$$

$$2SnO \rightarrow Sn + SnO_2 \tag{21}$$

$$Sn + 2H_2O \rightarrow SnO_2 + H_2 \tag{22}$$

Fan et al. [43] have studied steam to hydrogen conversion using six different metals. It is interesting to note that only Fe and Sn are found to generate reasonable hydrogen at 873 K as shown in Table 6. Other metals did not show a good amount of hydrogen production at 873 K. Considering melting point of different metallic and their oxides states (as shown in Table 7) of Fe and Sn it can be inferred that Fe is very suitable for given application unless there is a provision to handle liquid metal in the solar reactor similar to Zn–ZnO_2 case. The steam to H_2 value (γ^a) of 40.82 % is lower compared to one reported by Abanades et al. [15] which is equivalent to 90 % at similar conditions. If solar reactor is designed to handle liquid metals, then both Zn and Sn seems to be better candidates for two-step redox reactions with good hydrogen yield and at low-temperature operation.

Recently, Cho and Kim [27] reported production of H_2 using solid acids such as silica gel, activated Al_2O_3, $CaCO_3$, TiO_2 and ZnO. This is very interesting study as it reports on liberation of hydrogen gas at very low temperature. They have demonstrated the possibility of H_2 production using a laboratory plug flow reactor. Figure 7 gives

Table 6 Maximum per-pass conversion of H_2O to H_2 in the regeneration reactor and the stable phase obtained at 873 K for counter-current gas–solid operation

Metal phase	γ^a (%)	Oxidized phase
Ni	0.4	NiO
Cd	1.83	CdO
Cu	0	Cu_2O
Co	2.27	CoO
Sn	40.82	SnO_2
MnO	0	Mn_3O_4
Fe	74.79	Fe_3O_4
Fe	74.79	Fe_2O_3

γ^a conversion of H_2O to H_2

Table 7 Melting points [44] of various phases of Fe and Sn

Material	Melting point (K)
Fe (cast)	1,548
Fe (pure)	1,808
FeO	1,693
Fe_3O_4	1,538
Fe_2O_3	1,811
Sn	504
SnO	1,353
SnO_2	1,400

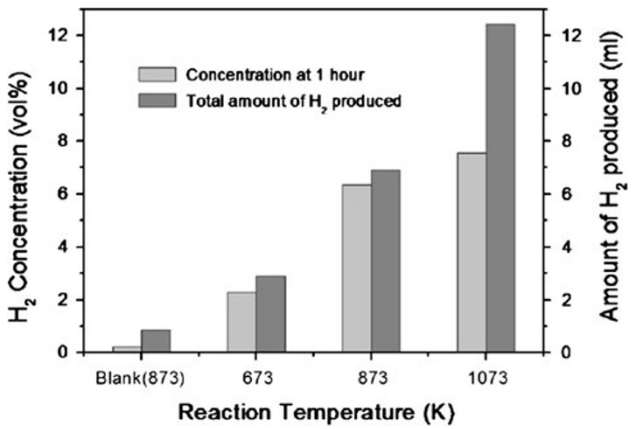

Fig. 7 H_2 concentration in the product gas stream at a reaction time of 1 h and total amount of H_2 produced versus reaction temperature resulted from using a wetted Al_2O_3. For the experiments, 60 g of Al_2O_3 (5.5 wt% H_2O) in a stainless steel reactor and 2 ml/min of CO_2 carrier gas were used at atmospheric pressure

the concentration and total amount of H_2 liberated at various temperatures using activated Al_2O_3.

The concentration of hydrogen produced in product gas stream using five different oxides at $\approx$610 K is shown in the Table 8. Though $CaCO_3$ shows highest concentration of H_2, i.e., 1,590 ppm in 1 h reaction time the activated Al_2O_3 produces highest amount of total H_2 at 1,073 K.

Though the authors demonstrated the workability of the producing hydrogen from solid acids on a laboratory-scale fixed-bed reactor, replication of the results in a solar reactor needs to be performed to know the feasibility of the process.

One of the main problem to tackle is overcoming sintering of redox material. Agglomeration due to sintering brings down the recyclability over multiple redox cycles. The key properties of the redox material should include a high oxygen carrying capacity, good mechanical properties and cheap and easy synthetic procedures. If redox material do not fulfill any one of these key properties it would not be a suitable material for commercial-scale operation.

Particle size or grain size effect on rate of oxidation

It is generally accepted that smaller the particle size easier is to oxidize or reduce. In case of two-phase alloys the rate of oxidation may significantly improve with grain size reduction because both mutual solubility and diffusivity among the system will enhance [45, 46]. But this is not always the case, during the oxidation if the top layer acts as a protective layer then the further oxidation of the metals will be hampered.

Figure 8 shows the oxidation kinetics of three different alloy systems with two different grain sizes at 1,073 K. The grain size reduced Cu–Cr alloy showed very slow oxidation kinetics compared to As-cast alloy. But in case of Cu–Fe and Cu–Co oxidation kinetics found to be much faster when nano-crystals (20–30 nm) were used compared to the As-cast alloy. This is because Cr_2O_3 scale formed on alloy prevents further oxidation. This is similar to in case aluminum where external layer forms Al_2O_3 and prevents further oxidation or corrosion of the aluminum metal.

The reduction kinetics of metal oxides depends on many factors such as whether they are supported or unsupported, particle size, gas atmosphere, kind of metal oxides and whether single or mixed metal oxides. There are not many reports available on high-temperature reduction of metal oxides in an inert atmosphere as in the case of solar thermal reduction, but there are plenty of studies available in the literature on reduction of metal oxides using H_2 or CO as reducing agents. For example, Syed-Hassan and Chun-Zhu [47] have studied the particle size effect on reduction of NiO in H_2 atmosphere. The reduction profiles for NiO particles of size 20 and 24 nm are very different from that of particle size of 3.3 nm (please refer Fig. 5a in Ref. [47]). The profiles for 20 and 24 nm are almost similar and very much resemble to that of 55 nm NiO supported on SiO_2 substrate. Authors concluded that reduction kinetics is independent of supported or unsupported NiO, but merely

Table 8 H_2 concentration in the product gas stream at a reaction time of 1 h

Solid acid (amount)	Al_2O_3 (50 g)		SiO_2 (30 g)		TiO_2 (50 g)		ZnO (50 g)		$CaCO_3$ (50 g)	
H_2O (wt%)	0	5.2	0	5.3	0	5.1	0	5.1	0	5.0
H_2 (ppm)	0	870	0	200	0	260	0	630	0	1,590

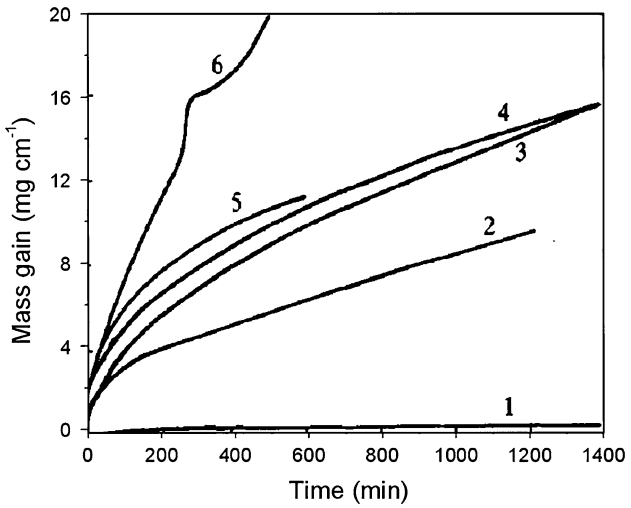

Fig. 8 Oxidation kinetics of As-cast and grain size reduced Cu–M alloys at 1,073 K. *1* Grain size reduced Cu–Cr alloy, *2* As-cast Cu–Co alloy, *3* As-cast Cu–Cr alloy, *4* grain size reduced Cu–Fe alloy, *4* As-cast Cu–Fe alloy, *6* grain size reduced Cu–Co alloy. [45]

depends on the particle/crystal size. The E_a versus %NiO converted trends are very different for first reduction (particle size 3.3 nm) to that of second (particle size = 20 nm) and third reduction (particle size = 24 nm) (please refer Fig. 5b in Ref. [47]). The E_a for first reduction remains almost unchanged (indicating single rate-limiting step) throughout the whole reduction process, but for second and third reduction steps the E_a profiles continuously increased till the complete reduction of NiO. The main reason for the difference could be due to the difference in surface to bulk atoms in different particle size crystals. The size of the metallic island which forms during initial stages of reduction is bigger than particle size, i.e., 3.3 nm, or the whole particle surface can be instantaneously covered by the metallic layer without requiring a significant growth of islands; therefore, the reduction happens immediately in those particles size crystals. But for a big particle with significant atoms in the interior (e.g., 20 nm) it might take quite some time for the growth of island to cover the whole particle's surface. Once the surface has been covered completely by the metal product, the Ni–NiO boundary would then progressively advance inward. As reduction continues, the hydrogen radicals moves towards Ni–NiO boundary on the surface and the diffusion of atoms (i.e., movement and rearrangements of atoms in the interior of the particle) takes place. In general, solid-state diffusion requires higher activation energy [48]. The number of steps of diffusion in the solid state would appear to increase with NiO conversion, resulting in continuous increases in the activation energy. This is the reason in general the reduction of bigger particles crystallites needs higher activation energy than smaller one.

Table 9 Hydrogen cost estimation (per kg H_2) in different processes

Years	Hy-S	CuCl	Ferrite	S–A	ZnO	CdO	MnO	S–I
2015	$5.68	$6.83	$4.06	$7.78	$6.07	NA	$	$
2025	$3.85	$5.39	$2.42	$4.71	$4.18	NA	$4.63	$4.68

Economic evaluation

The US DOE has established a target of $2 to $3 per kg hydrogen by 2025 to make it economically affordable. The short term, i.e., 2015, DOE target is $6/kg hydrogen. Any competitive technology to produce hydrogen considers this figure as a reference for their process efficiency and economic evaluation.

DOE in collaboration with TIAX (TIAX is a laboratory-based technology development company with a focus on clean energy) led the effort of cost calculation for solar thermochemical hydrogen (STCH) in many US national laboratories. They considered eight promising technologies for cost calculations, viz., hybrid-sulfur (HyS), copper chloride (CuCl), thin-film nickel ferrite ("ferrite"), sulfur-ammonia (S–A), zinc oxide (ZnO), manganese oxide (MnO), sulfur-iodine (S–I), and cadmium oxide (CdO).

Five out of eight technologies mentioned in Table 9 appear to meet DOE's short-term target (by 2015) of $6/kg hydrogen but meeting long-term target seems quite difficult. Only thin film ferrite is very close to DOE's long-term requirement. Even in this case achieving the long-term targets require significant technological advances in multiple dimensions. The primary cost driver for all the processes that were analyzed was heliostats costs. Reducing the heliostats cost or increase in plant efficiency will bring down the CAPEX and OPEX. Most probably mass production of heliostats and improving its efficiency will help to reduce the CAPEX and help to meet DOE hydrogen cost targets.

Conclusions

Several metal oxides have been proposed to apprehend redox cycles. To-date, the solar-to-fuel efficiencies of prototype reactors are low, on the order of <1 %. The main problem in large-scale solar application would be an efficient fast quenching system to hinder the reoxidation of the reduced metal in liquid or in vapor phase. When molten metal is made to react with steam, an oxide layer will form on the surface and it floats on top of the melt, which prevents further oxidation reaction.

So far, there are no reports demonstrating good repeatability of the cyclic two-step reaction to satisfy the practical use of the process. This would be one of the most difficult achievements in this technology because the high-temperature process will cause significant sintering of the metal oxide, which severely deactivates metal oxide for repeated cyclic reactions.

Though there are hundreds of publication available in the literature on metal oxide redox cycle for hydrogen production, only few of them are practically demonstrated in prototype solar reactor. The challenges while conducting redox experiments in a solar reactor are very different than in a laboratory-scale plug flow reactor. The commercial realization of redox technology for hydrogen production seems still far away.

Acknowledgments I thank SABIC CRI for giving me an opportunity to work on this review and publish; Dr. Hicham Idriss for his valuable input on the manuscript and Dr. Sandro Gambarotta for his constant support, guidance and encouragement.

References

1. Licht, S.: Solar water splitting to generate hydrogen fuel—a photothermal electrochemical analysis. Int. J. Hydrog. Energy **30**(5), 459–470 (2005)
2. Kogan, A.: Direct solar thermal splitting of water and on-site separation of the products—II. Experimental feasibility study. Int. J. Hydrog. Energy **23**(2), 89 (1998)
3. Lede, J., Villermaux, J., Ouzane, R., Hossain, M.A., Ouahes, R.: Production of hydrogen by simple impingement of a turbulent jet of steam upon a high temperature zirconia surface. Int. J. Hydrog. Energy **12**(1), 3–11 (1987)
4. Bilgen, E., Ducarroir, M., Foex, M., Sibieude, F., Trombe, F.: Use of solar energy for direct and two-step water decomposition cycles. Int. J. Hydrog. Energy **2**(3), 251–257 (1977)
5. Nakamura, T.: Hydrogen production from water utilizing solar heat at high temperatures. Sol. Energy **19**(5), 467 (1977)
6. Lundberg, M.: Model calculations on some feasible two-step water splitting processes. Int. J. Hydrog. Energy **18**(5), 369 (1993)
7. Palumbo, R., Léde, J., Boutin, O., Elorza Ricart, E., Steinfeld, A., Möller, S., Weidenkaff, A., Fletcher, E.A., Bielicki, J.: The production of Zn from ZnO in a high-temperature solar decomposition quench process—I. The scientific framework for the process. Chem Eng Sci **53**(14), 2503–2517 (1998)
8. Palumbo, R.: Solar thermal chemical processing: Challenges and changes. J Phys IV Fr **9**, Pr3-35–Pr33-40 (1999)
9. Weidenkaff, A., Brack, M., Möller, S., Palumbo, R., Steinfeld, A.: Solar thermal production of zinc: Program strategy and status of research. J Phys IV Fr **9**, Pr3-313–Pr3-318 (1999)
10. Sibieude, F., Ducarroir, M., Tofighi, A., Ambriz, J.: High temperature experiments with a solar furnace: The decomposition of Fe_3O_4, Mn_3O_4, CdO. Int. J. Hydrog. Energy **7**(1), 79–88 (1982)
11. Ehrensberger, K., Frei, A., Kuhn, P., Oswald, H.R., Hug, P.: Comparative experimental investigations of the water-splitting reaction with iron oxide $Fe_{1-y}O$ and iron manganese oxides $(Fe_{1-x}Mn_x)_{1-y}O$. Solid State Ionics **78**, 151–160 (1995)
12. Ehrensberger, K., Kuhn, P., Shklover, V., Oswald, H.R.: Temporary phase segregation processes during the oxidation of $(Fe_{0.7}Mn_{0.3})_{0.99}O$ in $N_2 + H_2O$ atmosphere. Solid State Ionics **90**, 75–81 (1996)
13. Tamaura, Y., Steinfeld, A., Kuhn, P., Ehrensberger, K.: Production of solar hydrogen by a novel, 2-step, water-splitting thermochemical cycle. Energy **20**(4), 325 (1995)
14. Steinfeld, A., Kuhn, P., Reller, A., Palumbo, R., Murray, J., Tamaura, Y.: Solar-processed metals as clean energy carriers and water-splitters. Int. J. Hydrog. Energy **23**(9), 767–774 (1998)
15. Abanades, S., Charvin, P., Lemont, F., Flamant, G.: Novel two-step SnO_2/SnO water-splitting cycle for solar thermochemical production of hydrogen. Int. J. Hydrog. Energy **33**(21), 6021 (2008)
16. Kaneko, H., Kodama, T., Gokon, N., Tamaura, Y., Lovegrove, K., Luzzi, A.: Decomposition of Zn-ferrite for O_2 generation by concentrated solar radiation. Sol. Energy **76**, 317 (2004)
17. Kodama, T., Nakamuro, Y., Mizuno, T.J.: A two-step thermochemical water splitting by iron-oxide on stabilized zirconia. J. Sol. Energy Eng. **128**, 3 (2006)
18. Kodama, T.: High-temperature solar chemistry for converting solar heat to chemical fuels. Prog. Energy Combust. Sci. **29**(6), 567 (2003)
19. Abanades, S., Flamant, G.: Thermochemical hydrogen production from a two-step solar-driven water-splitting cycle based on cerium oxides. Sol. Energy **80**(12), 1611 (2006)
20. Chueh, W.C., Falter, C., Abbott, M., Scipio, D., Furler, P., Haile, S.M., Steinfeld, A.: High-flux solar-driven thermochemical dissociation of CO_2 and H_2O using nonstoichiometric ceria. Science **330**(6012), 1797–1801 (2010)
21. Lapp, J., Davidson, J.H., Lipinski, W.: Efficiency of two-step solar thermochemical non-stoichiometric redox cycles with heat recovery. Energy **37**, 591–600 (2012)
22. Kaneko, H., Taku, S., Tamaura, Y.: Reduction reactivity of CeO_2–ZrO_2 oxide under high O_2 partial pressure in two-step water splitting process Sol. Energy **85**(9), 2321–2330 (2011)
23. Kang, K.-S., Kim, C.-H., Park, C.-S., Kim, J.-W.: Hydrogen reduction and subsequent water splitting of Zr-added CeO_2. J. Ind. Eng. Chem. **13**(4), 657–663 (2007)
24. SP Gal, A., Abanades, A.: Dopant incorporation in Ceria for enhanced water-splitting activity during solar thermochemical hydrogen generation. J. Phys. Chem. C **116**, 13516–13523 (2012)
25. Palumbo, R., Rouanet, A., Pichelin, G.: The solar thermal decomposition of TiO_2 at temperatures above 2200 K and its use in the production of Zn from ZnO. Energy **20**(9), 857–868 (1995)
26. Abanades, S., Charvin, P., Flamant, G., Neveu, P.: Screening of water-splitting thermochemical cycles potentially attractive for hydrogen production by concentrated solar energy. Energy **31**(14), 2805–2822 (2006)

27. Cho, Y.S., Kim, J.H.: Hydrogen production by splitting water on solid acid materials by thermal dissociation. Int. J. Hydrog. Energy **36**(14), 8192–8202 (2011)
28. Bilgen, E., Bilgen, C., Beghi, GE., Ducarroir, M.: Thermochemical hydrogen producing processes. Contract file No. 08SX.31155-8-6602. Prepared by Exergy Research Corporation, prepared for NRC of Canada, Montreal Road, Ottawa, KlA OR6, J.J. Murray (1979)
29. Tamaura, Y., Ueda, Y., Matsunami, J., Hasegawa, N., Nezuka, M., Sano, T., Tsuji, M.: Solar hydrogen production by using ferrites sol. Energy **65**(1), 55–57 (1999)
30. Loutzenhiser, P., Meier, A., Steinfeld, A.: Review of the two-Step H_2O/CO_2-splitting solar thermochemical cycle based on Zn/ZnO redox reactions. Materials **3**, 4922–4938 (2010)
31. Hed, A.Z., Tannhauser, D.S.: Contribution to the Mn-O phase diagram at high temperature. J. Electrochem. Soc. **4**, 314–318 (1967)
32. Rager, T.: Re-evaluation of the efficiency of a ceria-based thermochemical cycle for solar fuel generation. Chem. Commun. **48**, 10520–10522 (2012)
33. Inoue, M., Asegawa, N., Uehara, R., Gokon, N., Kaneko, H., Tamaura, Y.: Solar hydrogen generation with H_2O/ZnO/$MnFe_2O_4$ system. Sol. Energy **76**(1–3), 309–315 (2004)
34. Roeb, M., Sattle, C., Klüser, R., Monnerie, N., Oliveira, L.D., Al, E.: Solar hydrogen production by a two-step cycle based on mixed iron oxides. J. Sol. Energy Eng. Trans. ASME **128**(2), 125–133 (2006)
35. Kodama, T., Nakamuro, Y., Mizuno, T.: A two-step thermochemical water splitting by iron-oxide on stabilized zirconia. J. Sol. Energy Eng. Trans. ASME **128**(1), 3–7 (2006)
36. Gokon, N., Mizuno, T., Nakamuro, Y., Tamaura, K., Kodama, T.: Iron-containing yttria-stabilized zirconia system for two-step thermochemical water splitting. J. Sol. Energy Eng. Trans. ASME **130**(1), 011018 (2008)
37. Perkins, C., Weimer, A.W.: Likely near-term solar-thermal water splitting technologies. Int. J. Hydrog. Energy **29**(15), 1587–1599 (2004)
38. Steinfeld, A.: Solar hydrogen production via a two-step water-splitting thermochemical cycle based on Zn/ZnO redox reactions. Int. J. Hydrog. Energy **27**(6), 611 (2002)
39. Lédé, J., Elorza-Ricart, E., Ferrer, M.: Solar thermal splitting of zinc oxide: A review of some of the rate controlling factors. J. Sol. Energy Eng. Trans. ASME **123**(2), 91–97 (2001)
40. Haueter, P., Moeller, S., Palumbo, R., Steinfeld, A.: The production of zinc by thermal dissociation of zinc oxide—Solar chemical reactor design. Sol. Energy **67**(1–3), 161–167 (1999)
41. Perkins, C., Lichty, P.R., Weimer, A.W.: Thermal ZnO dissociation in a rapid aerosol reactor as part of a solar hydrogen production cycle. Int. J. Hydrog. Energy **33**(2), 499–510 (2008)
42. Souriau, D.: Procédé et dispositif pour l'utilisation d'énergie thermique à haute température, en particulier d'origine nucléaire. Device and method for the use of high temperature heat energy, in particular of nuclear origin. France Patent FR2135421
43. Gupta, P., Velazquez-Vargas, L.G., Fan, L.S.: Syngas redox (SGR) process to produce hydrogen from coal derived syngas. Energy Fuels **21**(5), 2900–2908 (2007)
44. Perry, R.H., Green, D.: Perry's Chemical Engineers Handbook, 6th edn. McGraw-Hill, New York (1984)
45. Yuan-shi, L., Yan, N., Guang-yan, F., Wei-tao, W., Gesmundo, F.: Effect of grain size reduction on high temperature oxidation of binary two-phase alloys. Trans. Nonferrous Met. Soc. China **11**(5), 644–648 (2001)
46. Zhong-qiu, C., Yan, N., Li-Jie, C., Wei-tao, W.: Effect of grain size reduction on high temperature oxidation of behaviour of Cu-80Ni alloy. Trans. Nonferrous Met. Soc. China **13**(4), 908–911 (2003)
47. Syed-Hassan, S.S.A., Li, C.-Z.: Effects of crystallite size on the kinetics and mechanism of NiO reduction with H_2. Int. J. Chem. Kinet. **43**(12), 667–676 (2011)
48. Mrowec, S.: Defects and Diffusion in Solids: An Introduction. Elsevier, Amsterdam (1980)